

Article

# The Pluripotency Factor Nanog Protects against Neuronal Amyloid $\beta$ -Induced Toxicity and Oxidative Stress through Insulin Sensitivity Restoration

Ching-Chi Chang <sup>1,2,†</sup>, Hsin-Hua Li <sup>1,3,†</sup>, Sing-Hua Tsou <sup>1</sup>, Hui-Chih Hung <sup>4</sup>,  
Guang-Yaw Liu <sup>1</sup>, Tatiana A. Korolenko <sup>5</sup>, Te-Jen Lai <sup>1,2</sup>, Ying-Jui Ho <sup>6,\*</sup> and Chih-Li Lin <sup>1,3,\*</sup>

<sup>1</sup> Institute of Medicine, Chung Shan Medical University, Taichung 402367, Taiwan; fmaj7@seed.net.tw (C.-C.C.); vivid529@hotmail.com (H.-H.L.); zinminid@gmail.com (S.-H.T.); liugy@csmu.edu.tw (G.-Y.L.); tejenlai@hotmail.com (T.-J.L.)

<sup>2</sup> Department of Psychiatry, Chung Shan Medical University Hospital, Taichung 402367, Taiwan

<sup>3</sup> Department of Medical Research, Chung Shan Medical University Hospital, Taichung 402367, Taiwan

<sup>4</sup> Department of Life Sciences and Institute of Genomics and Bioinformatics, National Chung Hsing University, Taichung 402204, Taiwan; hchung@dragon.nchu.edu.tw

<sup>5</sup> Scientific Research Institute of Physiology and Basic Medicine, Novosibirsk 630117, Russia; t.a.korolenko@physiol.ru

<sup>6</sup> Department of Psychology, Chung Shan Medical University, Taichung 402367, Taiwan

\* Correspondence: yjho@csmu.edu.tw (Y.-J.H.); dll@csmu.edu.tw (C.-L.L.);  
Tel.: +886-4-2473-0022-11673 (Y.-J.H.); +886-4-2473-0022-11690 (C.-L.L.)

† The first two authors contributed equally to this work.

Received: 12 May 2020; Accepted: 25 May 2020; Published: 27 May 2020



**Abstract:** Amyloid  $\beta$  ( $A\beta$ ) is a peptide fragment of the amyloid precursor protein that triggers the progression of Alzheimer's Disease (AD). It is believed that  $A\beta$  contributes to neurodegeneration in several ways, including mitochondria dysfunction, oxidative stress and brain insulin resistance. Therefore, protecting neurons from  $A\beta$ -induced neurotoxicity is an effective strategy for attenuating AD pathogenesis. Recently, applications of stem cell-based therapies have demonstrated the ability to reduce the progression and outcome of neurodegenerative diseases. Particularly, Nanog is recognized as a stem cell-related pluripotency factor that enhances self-renewing capacities and helps reduce the senescent phenotypes of aged neuronal cells. However, whether the upregulation of Nanog can be an effective approach to alleviate  $A\beta$ -induced neurotoxicity and senescence is not yet understood. In the present study, we transiently overexpressed Nanog—both in vitro and in vivo—and investigated the protective effects and underlying mechanisms against  $A\beta$ . We found that overexpression of Nanog is responsible for attenuating  $A\beta$ -triggered neuronal insulin resistance, which restores cell survival through reducing intracellular mitochondrial superoxide accumulation and cellular senescence. In addition, upregulation of Nanog expression appears to increase secretion of neurotrophic factors through activation of the Nrf2 antioxidant defense pathway. Furthermore, improvement of memory and learning were also observed in rat model of  $A\beta$  neurotoxicity mediated by upregulation of Nanog in the brain. Taken together, our study suggests a potential role for Nanog in attenuating the neurotoxic effects of  $A\beta$ , which in turn, suggests that strategies to enhance Nanog expression may be used as a novel intervention for reducing  $A\beta$  neurotoxicity in the AD brain.

**Keywords:** amyloid  $\beta$ ; insulin signaling; oxidative stress; Nanog; senescence

## 1. Introduction

Alzheimer's disease (AD) is a common neurodegenerative disease accounting for half of all dementia cases. Although the pathogenesis of AD is quite complex and not fully understood,

the increase of extracellular senile plaques in the brain acts as a central hallmark of disease progression. It is known that the major protein component of the senile plaques is a short peptide called amyloid  $\beta$  ( $A\beta$ ) which causes neuronal cell death and thus leading to dementia [1]. Although several toxic pathways were implicated, it is known that  $A\beta$  plays a causative role of mitochondrial dysfunction and oxidative stress that in turn leads to neuronal dysfunction and apoptosis [2]. The deposition of  $A\beta$  is a significant pathologic feature seen in the aging brain [3], indicating  $A\beta$  may accelerate neuronal senescence [4]. In particular, the dysregulation of mitochondrial turnover is involved in brain senescence, demonstrating that impairment of mitochondrial function and increased oxidative damage also play an important role in AD-related pathology [5]. Actually, there is strong evidence that the greatest risk factor for AD is the increasing age [6]. This indicates therapeutic strategies to reduce  $A\beta$  toxicity can focus on slowing down or reversing the effects of neuronal aging [7]. Emerging evidence suggests that neuron aging is affected by the cell microenvironment and elicited by  $A\beta$  accumulation, which was shown to induce cellular senescence via generation of excessive levels of reactive oxygen species (ROS) [8]. In contrast, the potential of stem cell-based approaches in slowing down the aging process is relevant for neuroprotection in AD [9]. For, example, stem cells were demonstrated to serve as a protective source for neurotrophic factors secretion in attenuating  $A\beta$ -induced cytotoxicity and apoptosis [10]. Therefore, safeguarding the survival of neuronal cells by enhancing specific stemness gene expression may play a role in reducing toxic impact of  $A\beta$  in the brain.

It is known that type 2 diabetes (T2D) is another important non-genetic risk factor of AD, suggesting that alterations in insulin signaling may also be involved in AD pathogenesis [11]. In fact, recent studies have confirmed that insulin signaling is indeed impaired in the AD brain [12]. Particularly, impairments in brain insulin signaling transduction is associated with  $A\beta$  accumulation [13], indicating  $A\beta$  may contribute to brain insulin resistance. Previously, we have demonstrated that a pluripotency-associated miRNA miR-302 plays a neuroprotective role against  $A\beta$  toxicity [14]. We reported that the upregulation of miR-302 can suppress  $A\beta$ -induced insulin signaling blockade and maintain the intracellular redox balance toward cell survival. In addition, miR-302 also alleviated  $A\beta$ -mediated mitochondrial dysfunction thus diminishing oxidative and senescence-associated damages in neuronal cells. Interestingly, our data also revealed that genetic or pharmacologic stimulation of miR-302 upregulates high Nanog expression. Since Nanog is known as a transcriptional factor that enhances self-renewal, pluripotency [15] and antiaging [16] in stem cell biology, it is likely that Nanog itself may contribute to protect neuronal cells against  $A\beta$  toxicity. However, whether the upregulation of Nanog can be an effective way to reduce  $A\beta$  neurotoxicity is not yet understood. Therefore, in this study we investigated the protective mechanisms of Nanog. Our results showed that overexpression of Nanog is responsible for attenuating  $A\beta$ -triggered neuronal insulin resistance, which promotes cell survival through reducing intracellular ROS production and cellular senescence. This indicates upregulation of Nanog may promote survival of neuronal cells by attenuating  $A\beta$  neurotoxicity.

## 2. Materials and Methods

### 2.1. Materials

The human wild-type Nanog (#28221) expression vector was acquired from Addgene (Cambridge, MA, USA). All chemicals were purchased from Sigma (München, Germany). Primary antibodies used in this study:  $\beta$ -actin (NB600-501), Akt (sc-8312), p-Akt (sc-33437), GSK3 $\beta$  (sc-8257), p-GSK3 $\beta$  (sc-11757), Nrf2 (sc-722), caspase 3 (sc-7148) and poly (ADP-ribose) polymerase (PARP) (sc-7150) were obtained from Santa Cruz Biotechnology (Santa Cruz, CA, USA); SOD1 (#2770S) and Sirt1 (GTX61042) were purchased from GeneTex (Irvine, CA, USA); tau (05-348), p-tau (MAB5450) and p-Tyr (05-321) were obtained from Millipore (Bedford, MA, USA); Nanog (#4903), IRS-1 (194320) and p-IRS-1 (05-1087) were purchased from Cell Signaling Technology (Danvers, MA, USA).  $A\beta_{1-42}$  was synthesized by LifeTein (Somerset, NJ, USA) and soluble  $A\beta$  oligomers were prepared according to our previously described [17]. Briefly,  $A\beta$  was first dissolved in hexafluoroisopropanol (HFIP), distributed in aliquots,

dried and stored at  $-80^{\circ}\text{C}$ . The day before the experiment,  $\text{A}\beta$  was dissolved in sterile dimethyl sulfoxide (DMSO), then diluted with PBS (pH 7.4) at a final concentration of  $100\ \mu\text{M}$ , vortexed and incubated at  $4^{\circ}\text{C}$  for 24 h.

## 2.2. Cell Culture, Transfection and Viability Assay

SK-N-MC cells (human neuroblastoma cell line) were obtained from the American Type Culture Collection (Bethesda, MD, USA). Cells were cultured in Minimal Eagle's Medium (MEM; Gibco) supplemented with 10% fetal calf serum, antibiotics (100 units/mL penicillin,  $100\ \mu\text{g}/\text{mL}$  streptomycin), 2-mM L-glutamine and kept in a humidified air containing 5%  $\text{CO}_2$  at  $37^{\circ}\text{C}$ . Transient transfections were carried out using Lipofectamine 3000 reagent (Thermo Fisher Scientific, Waltham, MA, USA), according to manufacturer's instruction. For viability assays, cells were treated with tetrazolium salt methyl-thiazol-tetrazolium (MTT) for 30 min, and then analyzed spectrophotometrically at 550 nm. Viability was determined as percent of control cells treated with vehicle alone.

## 2.3. mRNA Expression Analysis by Reverse-Transcription Quantitative PCR (qPCR)

Total mRNA was extracted from cultured cells or rat brain tissues using RNeasy Kit (Qiagen, Germantown, MD, USA). mRNAs were reverse-transcribed into cDNAs using TProfessional Thermocycler Biometra (Göttingen, Germany) following the manufacturer's recommendations. qPCR was performed on an ABI 7300 Sequence Detection System (Applied Biosystems, Foster City, CA, USA), using Power SYBR Green PCR Master Mix (Applied Biosystems). The following temperature parameters were used: initial denaturation at  $95^{\circ}\text{C}$  for 10 min, 40 cycles of denaturation at  $95^{\circ}\text{C}$  for 15 s, annealing at  $60^{\circ}\text{C}$  for 1 min and dissociation stage at  $95^{\circ}\text{C}$  for 15 s,  $60^{\circ}\text{C}$  for 15 s and  $95^{\circ}\text{C}$  for 15 s. The following primer pairs were used: forward 5'-GACGT GTGAA GATGA GTGAA ACTGA-3' and reverse 5'-GTTTC CAAAC AAGAA AAATC CTATG AG-3' for Nanog, forward 5'-GCTGG CGATT CATAA GGATA GAC-3' and reverse 5'-TATAC AACAT AAATC CACTA TCTTC CCCT-3' for brain-derived neurotrophic factor (BDNF), forward 5'-TGCTT CCGGA GCTGT GATCT-3' and reverse 5'-CGGAC AGAGC GAGCT GACTT-3' for insulin-like growth factor 1 (IGF-1). The mRNA levels were normalized to glyceraldehyde 3-phosphate dehydrogenase (GAPDH) using primer pairs with forward 5'-TGGTAT CGTGG AAGGA CTCAT GAC-3' and reverse 5'-ATGCC AGTGA GCTTC CCGTT CAGC-3'. Each cDNA sample was tested in triplicate. Values of relative mRNA expression were obtained by using Sequence Detection Systems software (Sequence Detection Systems 1.2.3-7300 Real-Time PCR System; Applied Biosystems) with a cycle threshold ( $\Delta\Delta\text{Ct}$ ) method.

## 2.4. Western Blot Analysis

Whole extracts of cells and rat brain tissues were prepared using Gold Lysis buffer (50-mM Tris-HCl, pH 8.0, 5-mM ethylenediaminetetraacetic acid, 150-mM NaCl, 0.5% Nonidet P-40, 0.5-mM phenylmethylsulfonyl fluoride and 0.5-mM dithiothreitol). Equal protein amounts from whole lysates were separated by 8–10% sodium dodecyl sulfate (SDS)-polyacrylamide gel electrophoresis and then transferred to polyvinylidene difluoride membranes (Millipore). The membranes were probed with primary antibodies followed by secondary antibodies conjugated with horseradish peroxidase. Images were acquired using Amersham ECL reagents and AI600 imager system (GE Healthcare, Chicago, IL, USA).

## 2.5. DAPI Staining on Nuclei

Cells were fixed in ice-cold methanol with 4% paraformaldehyde for 24 h. After that cells were incubated with 4',6-diamidino-2-phenylindole (DAPI) solution ( $1\ \text{ng}/\text{mL}$  in McIlvaine's buffer, pH 7.0) for 15 min at room temperature and observed with a fluorescent microscope (DP80/BX53, Olympus, Tokyo, Japan) for apoptotic fragmented nuclei.

### 2.6. Detection of Superoxide by Dihydroethidium (DHE) Staining

DHE is a cell-permeable fluorogenic probe that reacts with superoxide to form ethidium and emits red fluorescence. At the end of experiments, cells were rinsed with PBS solution and then incubated in fresh media containing 10- $\mu$ M DHE solution for 30 min in the dark at room temperature. After incubation, cells were washed twice with PBS and observed by using an inverted fluorescence microscope (DP72/CKX41, Olympus). All images were used the same fluorescent conditions and exposure time.

### 2.7. Analysis of Mitochondrial Membrane Potential by JC-1 Staining

Cells were incubated with fresh media containing 1  $\mu$ M JC-1 and at 37 °C for 30 min. At the end of incubation, cells were washed to remove the staining medium. Fluorescence images were collected by using an inverted fluorescence microscope (DP72/CKX41, Olympus), and results were represented by the ratio of average red/green fluorescence intensity. Image Pro Plus 6.0 (Media Cybernetics, Rockville, MD, USA) software was used to measure red and green fluorescence and five random non-adjacent fields in each group were used for statistical analysis.

### 2.8. SA- $\beta$ -Galactosidase Staining

Cells were rinsed with 1-mM MgCl<sub>2</sub> in PBS (pH 6.0) and then stained for SA- $\beta$ -galactosidase using a senescence  $\beta$ -galactosidase staining kit (Cell Signaling Technology, Danvers, MA, USA) according to the manufacturer's instructions. After that, cells were washed twice with PBS and images were taken using a microscope (BX53, Olympus). SA- $\beta$ -galactosidase positive cells were quantified by counting five random non-adjacent fields in each group.

### 2.9. Experimental Animals

12-week-old male Wistar rats were kept on a 12:12-h light/dark cycle with light from 7 a.m. to 7 p.m. and housed individually with free access to food and water. Rats were randomly divided into four groups, with six rats for each group. All animal experiments were approved by the Institutional Animal Care and Use Committee of Chung Shan Medical University, Taiwan (CSMU No. 2086) and performed in accordance with the guidelines and regulations of the Institutional Animal Care and Use Committee. In Nanog overexpression studies, the human wild-type Nanog coding sequence was amplified and cloned into the recombinant adeno-associated viral serotype 2 (rAAV2) vector. Intracerebral injection protocol and vector preparation were in reference to our previous studies [18]. For stereotaxic intracerebroventricular (i.c.v.) injections, rats were anesthetized with Zoletil (10 mg/kg, i.p.; Vibac Laboratories, Carros, France) and mounted in a stereotaxic frame (Stoelting Co., Ltd., Chicago, IL, USA). The rAAV-Nanog vector solution of 10  $\mu$ L was injected into the left lateral cerebral ventricle with the following coordinates, 0.8 mm posterior to the bregma, 1.5 mm lateral from the midline and 3.8 mm ventral from the skull. A $\beta$ <sub>1-42</sub> solution of 5  $\mu$ L (2  $\mu$ g/ $\mu$ L, 10  $\mu$ g each side) was injected into each side of hippocampus CA2 by using the following stereotaxic coordinates: 2.8 mm posterior to the bregma, 2.6 mm left/right to the midline and 3.0 mm ventral to the bregma. All the injections were performed within 5 min and following the needle remained in the target location for 10 min to avoid reflux along the needle tract. After 6 weeks of intracerebral injection, behavioral testing was performed. After that the animals were sacrificed. Brains were dissected and collected and then homogenized and fixed immediately.

### 2.10. T-Maze Test and Object Recognition Behavior Tests

Working memory was assessed using a T-maze test. The rats learned to find food rewards in the T-maze using their working memory, and the percentage of correct responses and time latency were recorded. After 6 weeks of injection, rats were subjected to behavioral tests performed as per our previous studies [19]. Each rat underwent two training sessions (on days 1 and 2) and one test

session (on day 3); each training session consisted of nine trials. For object recognition tests, each rat was subjected to three exposure sessions at 24 h intervals (during days 4–6). Four different objects that were novel to the rats were presented before the experiment. Each rat was allowed to explore the objects in the open box for 5 min on three consecutive days. After 5 min of the last exposure session, one of the old objects was replaced by a novel one, and the animal was returned to the open box for a 5-min test session. Times spent exploring objects during exposure and test sessions were recorded. All data were collected by a SMART video tracking system (SMART v3.0, Panlab SL, Barcelona, Spain).

### 2.11. Statistical Analysis

All data are presented as means  $\pm$  standard error of the mean ( $\pm$ SEM). Unpaired Student's *t*-test performed correlations between two groups. For multiple comparisons, data were analyzed by one-way ANOVA with Dunnett's post hoc multiple comparisons. *F*, *DFn*, *DFd* and *p* indicated the value of the *F*-test, the degrees of freedom of the numerator and denominator and the significance, respectively. Each group was compared with the indicated group. Data were analyzed by SPSS v25.0 statistical software (SPSS, Inc., Chicago, IL, USA). Differences were considered statistically significant while using \* attached to indicate  $p < 0.05$  and \*\* to indicate  $p < 0.01$ .

## 3. Results

### 3.1. Overexpression of Nanog Significantly Reduced A $\beta$ -Mediated Cytotoxicity

To evaluate whether Nanog plays a role in enhancing neuroprotective effects against A $\beta$  toxicity, we transiently transfected SK-N-MC neuronal cells with Nanog overexpression vector. Figure 1a confirms the results of qPCR that Nanog-transfected cells expressed markedly a higher Nanog mRNA level compared to mock-transfected cells ( $p < 0.01$ ), indicating a successful overexpression of Nanog in SK-N-MC cells. western blot analysis also confirmed a significant induction of Nanog protein expression in transfected cells (Figure 1b). We next investigated whether overexpression of Nanog exerts protective effects against A $\beta$ -induced neuronal death. As shown in Figure 1c by phase-contrast microscopy, treated with A $\beta$  for 24 h caused marked cell death, whereas the overexpression of Nanog seemed to promote cell survival. Accordingly, MTT assays showed that treatment of cells with A $\beta$  reduces cell viability in mock-transfected cells. Conversely, this cytotoxicity was significantly attenuated by Nanog overexpression ( $F(3, 12) = 14.07$ ,  $p < 0.01$ , Figure 1d). To further determine which mode of cell death is induced by A $\beta$ , results of DAPI staining showed that incubation of cells with A $\beta$  appears to increase apoptotic nuclei fragmentation ( $F(3, 16) = 22.51$ ,  $p < 0.01$ , Figure 1e). Similarly, alternative approaches by western blotting demonstrated that A $\beta$  markedly increased cleavage of caspase 3 and poly (ADP-ribose) polymerase (PARP), two typical markers of apoptosis as shown in Figure 1f. However, these A $\beta$ -induced apoptotic changes were effectively suppressed by overexpression of Nanog, suggesting Nanog overexpression significantly reduced A $\beta$ -mediated cytotoxicity.

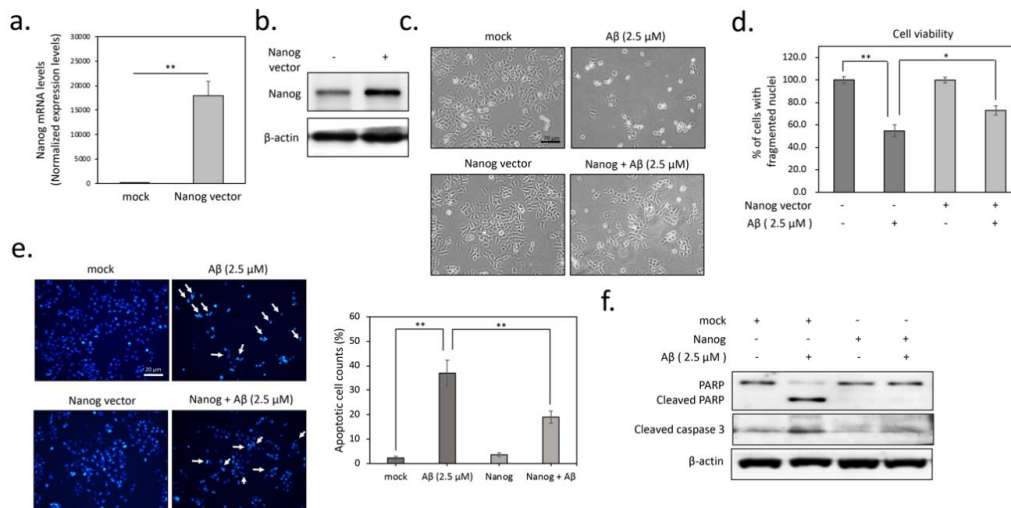


**Figure 1.** Overexpression of Nanog suppresses A $\beta$ -induced apoptosis in human neuronal cells (SK-N-MC). Quantification of Nanog expression using real-time PCR (a) and western blot (b). At 24 h post-transfection, both mRNA and protein levels of Nanog were significantly upregulated, indicating the successful overexpression of Nanog; (c) treatment with 2.5  $\mu$ M of A $\beta$ <sub>1–42</sub> for 24 h markedly induced morphologic changes and cell death and overexpression of Nanog prevented these effects by A $\beta$ ; (d) tetrazolium salt methyl-thiazol-tetrazolium (MTT) assays demonstrated that overexpression of Nanog significantly protected against A $\beta$ -induced cytotoxicity; (e) overexpression of Nanog markedly reduced A $\beta$ -induced nucleus fragmentation, determined using 4',6-diamidino-2-phenylindole (DAPI) staining. The percentage of apoptotic cells was calculated from five random fields; (f) western blotting results revealed that overexpression of Nanog inhibited A $\beta$ -induced caspase-3 and polymerase (PARP) cleavages, two hallmarks of apoptosis. Values were expressed as means  $\pm$  SEM from at least three independent experiments. The significance of differences was determined through unpaired Student's *t*-test or multiple comparisons with Dunnett's post hoc test at \*  $p < 0.05$  and \*\*  $p < 0.01$  compared with the indicated groups. Scale bar represents 20  $\mu$ m.

### 3.2. The Protection from A $\beta$ -Induced Apoptosis by Nanog is Dependent on Insulin Signaling in SK-N-MC Neuronal Cells

Our previous study has shown that A $\beta$  toxicity is involved in the blockade of insulin signaling in neuronal cells [14]. To determine whether overexpression of Nanog prevents A $\beta$ -impaired neuronal insulin signaling, we performed western blotting to detect the level of insulin receptor substrate 1 (IRS-1) phosphorylation at Ser<sup>307</sup>, a typical marker linked to the severity of insulin resistance. As shown in Figure 2a, the serine-phosphorylated IRS-1 increased in cells with 2.5  $\mu$ M A $\beta$  treatment for 24 h, suggesting neuronal insulin signaling transduction is impaired by A $\beta$ . Conversely, overexpression of Nanog caused a markedly decreased expression of serine-phosphorylated IRS-1. Similar results were also noted for tyrosine phosphorylation of IRS-1 that overexpression of Nanog dramatically enhances it in A $\beta$ -treated group. Since the marker of insulin resistance was observed to be changed, in the next step we investigated if Nanog would affect downstream Akt activity. As shown in Figure 2b, Akt Ser<sup>473</sup> phosphorylation was greatly diminished by A $\beta$ . However, the reduced Akt Ser<sup>473</sup> phosphorylation could be restored by overexpression of Nanog, suggesting Nanog can reverse A $\beta$ -induced neuronal insulin signaling blockade. It is known that the phosphorylation at the residue Ser<sup>9</sup> of glycogen synthase kinase 3 $\beta$  (GSK3 $\beta$ ) by Akt can inhibit its kinase activity and the inhibition of GSK3 $\beta$  reduces tau hyperphosphorylation [20]. To elucidate the protective effect of Nanog against A $\beta$ -induced cell death, the Ser<sup>9</sup> phosphorylation levels of GSK3 $\beta$  were also evaluated. The results showed that the Ser<sup>9</sup> phosphorylation of GSK3 $\beta$  was markedly suppressed by A $\beta$ , indicating A $\beta$ -inhibited IRS-1/Akt pathway results in GSK3 $\beta$  activation. However, the A $\beta$ -blocked Ser<sup>9</sup> GSK3 $\beta$  phosphorylation can be reversed by Nanog overexpression. This Nanog-mediated protection was also confirmed by inhibiting tau Thr<sup>231</sup> phosphorylation—a crucial pathologic hallmark of AD (Figure 2c). In order to further

investigate the role of IRS-1/Akt signaling in Nanog-mediated neuroprotection, the PI3-kinase inhibitor LY294002 was used as a negative control. As demonstrated in Figure 2d, LY294002 significantly blocked Nanog-prevented cell death by A $\beta$ . MTT viability assays also displayed similar results that LY294002 significantly reduces the protective effects of Nanog ( $F(2, 9) = 13.49, p < 0.01$ , Figure 2e). Accordingly, the results of DAPI staining and western blots demonstrated that LY294002 downregulates the anti-apoptotic efficacy of Nanog (Figure 2f,g). Taken together, these results suggest that overexpression of Nanog effectively represses A $\beta$ -induced tau phosphorylation and apoptosis by returning neuronal insulin signaling.

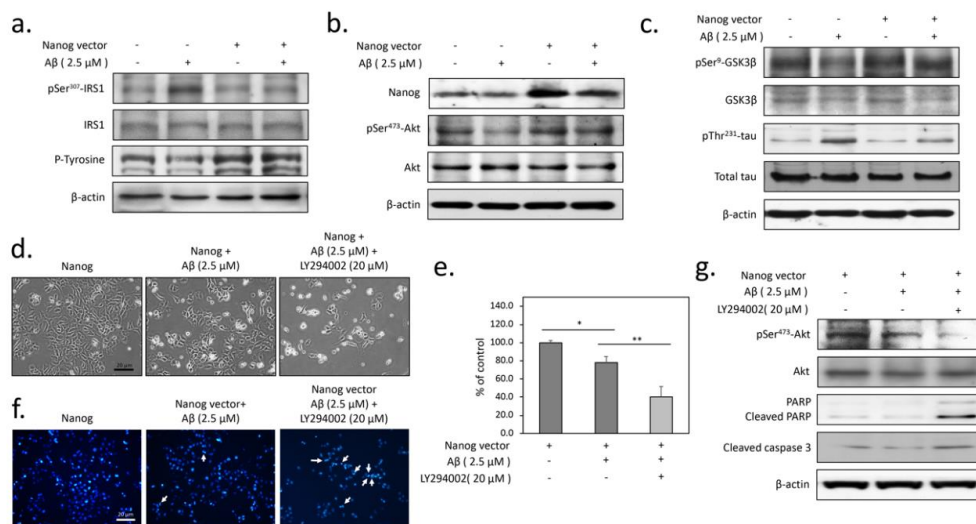


**Figure 2.** Overexpression of Nanog inhibits A $\beta$ -induced tau phosphorylation and cytotoxicity by restoring impaired insulin signaling; (a) western blots showed that treatment with 2.5  $\mu$ M of A $\beta$  for 24 h induces a marked increase of insulin receptor substrate 1 (IRS-1) Ser<sup>307</sup> phosphorylation, a major marker of insulin resistance. However, overexpression of Nanog greatly inhibited this phosphorylation; (b) western blot analysis of Ser<sup>473</sup> phosphorylated Akt confirmed that overexpression of Nanog reverses A $\beta$ -induced insulin signaling blockade; (c) western blot results indicated that overexpression of Nanog inhibits A $\beta$ -induced tau phosphorylation at Thr<sup>231</sup> and increases the phosphorylation of glycogen synthase kinase 3 $\beta$  (GSK3 $\beta$ ) at Ser<sup>9</sup>; (d) Bright field images showed that Nanog-induced protection is abolished by the co-treatment with LY294002 (20  $\mu$ M), a specific inhibitor of PI3-kinase; (e) MTT assays showed the LY294002 co-treatment inhibits the protective effect of Nanog; (f) LY294002 markedly reduced Nanog-induced anti-nucleus fragmentation effects determined by using DAPI staining. The arrows indicated apoptotic cells with nuclear fragmentation; (g) western blots showed that LY294002 markedly prevents the reduction of caspase-3 and PARP cleavages, suggesting the protection by Nanog is dependent on insulin signaling. Values were expressed as means  $\pm$  SEM from at least three independent experiments. The significance of differences was determined through multiple comparisons with Dunnett's post hoc test at \*  $p < 0.05$  and \*\*  $p < 0.01$  compared with the indicated groups. Scale bar represents 20  $\mu$ m.

### 3.3. A $\beta$ -Induced Superoxide Accumulation and Mitochondrial Dysfunction are Attenuated by Nanog Overexpression

Upon the basis of the above findings, we suggested that the protective effect of Nanog against A $\beta$  is likely related to the restoration of insulin signaling blockade in neuronal cells. Therefore, we investigated whether Nanog protects cells from A $\beta$ -induced oxidative stress by using the superoxide indicator dihydroethidium (DHE). As shown in Figure 3a, treatment with A $\beta$  for 16 h caused a marked increase of superoxide accumulation and this increase was counteracted by overexpression of Nanog. It is known that the cellular redox state is mainly regulated by nuclear factor erythroid 2-related factor 2 (Nrf2), which can stimulate the expression levels of endogenous antioxidant enzymes such as superoxide dismutase 1 (SOD1) [21]. As expected, western blot results demonstrated that overexpression of Nanog effectively restores A $\beta$ -induced reduction of Nrf2 and SOD1 levels (Figure 3b). However, co-treatment with LY294002 markedly attenuated Nanog-associated antioxidative effects including superoxide downregulation and Nrf2/SOD1 restoration, suggesting the involvement of insulin signaling in Nanog-mediated antioxidant activity. Because A $\beta$ -induced mitochondrial dysfunction is known to cause oxidative damage in neurodegeneration [22], the role of Nanog in preventing A $\beta$ -mediated impairment of mitochondrial membrane potential was also investigated. As shown in Figure 3c, A $\beta$  treatment resulted in a strong increase in green fluorescence, indicating a great loss of mitochondrial membrane potential by A $\beta$ . On the contrary, overexpression Nanog restored mitochondrial membrane potential significantly, suggesting Nanog preserves mitochondrial function against A $\beta$ -induced mitochondrial dysfunction. Accordingly, this restoration was attenuated by co-treatment of LY294002, implying again that insulin signaling is required for the antioxidative actions of Nanog. Some evidence suggests that A $\beta$ -induced oxidative stress mediates cellular senescence and contributes to AD pathogenesis [23]. As IGF-1 and BDNF exert a critical role of neurotrophins for survival of aged neurons that are degenerated in AD [24,25], we performed qPCR assays to determine differences in gene expressions with or without Nanog transfection. As shown in Figure 3d overexpression of Nanog upregulated both IGF-1 and BDNF mRNA expression, and this upregulation remained relatively high under A $\beta$  treatment, suggesting that Nanog-transfected cells may increase neurotrophic factors production and improve neuronal insulin resistance caused by A $\beta$  ( $F_{\text{IGF-1}}(4, 15) = 6.05, p < 0.05$ ;  $F_{\text{BDNF}}(4, 15) = 13.49, p < 0.01$ ). To elucidate whether Nanog can attenuate A $\beta$ -induced cellular senescence, we performed SA- $\beta$ -gal staining which is a common biomarker used in detecting senescent cells. The results of Figure 3e revealed a significant increase of SA- $\beta$ -galactosidase positive cells in A $\beta$ -treated cells, whereas Nanog effectively reduced the number of senescent cells (red arrows). Accordingly, A $\beta$  (1.25  $\mu$ M) caused a marked decrease in the expression of sirtuin-1 (Sirt1), a protein deacetylase that antagonizes cellular senescence (Figure 3f). This inhibition was effectively restored by overexpression of Nanog and abolished by combined treatment with LY294002. Collectively, our results indicate that restoration of mitochondrial function by Nanog may help reduce superoxide accumulation and protect neuronal cells from A $\beta$ -induced senescence.

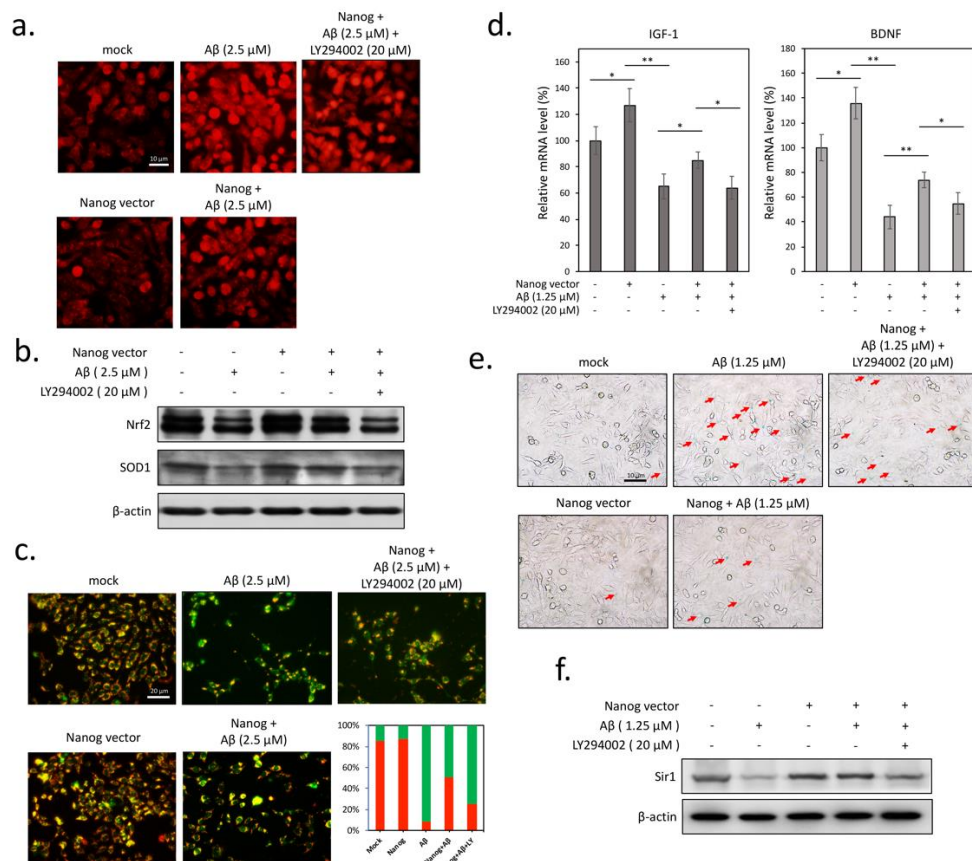


**Figure 3.** Nanog overexpression ameliorates Aβ-induced mitochondrial superoxide accumulation and cellular senescence. (a) Dihydroethidium (DHE) staining results showed that overexpression of Nanog reduces Aβ-induced intracellular superoxide accumulation; (b) levels of two antioxidant signaling-related proteins nuclear factor erythroid 2-related factor 2 (Nrf2) and superoxide dismutase 1 (SOD1) were analyzed by western blotting; (c) double fluorescence staining of mitochondrial membrane potential by JC-1 was used for detection of mitochondrial membrane potential. Green fluorescence indicated the decreased membrane potential in 2.5 μM of Aβ-treated SK-N-MC cells after 24 h. Red fluorescence indicated that overexpression of Nanog effectively preserves the mitochondrial membrane potential; (d) mRNA levels of neurotrophic factors insulin-like growth factor 1 (IGF-1) and brain-derived neurotrophic factor (BDNF) were measured by performing qPCR. mRNA levels of IGF-1 and BDNF were significantly increased in Aβ treated Nanog-overexpressed cells; (e) representative results of cytochemical detection of SA-β-galactosidase, a common biomarker used in detecting senescent cells. Senescent cells (red arrows) are blue stained under a bright-field microscope; (f) levels of sirtuin-1 (Sirt1) protein in Aβ-treated cells using western blotting. Values were expressed as means ± SEM from at least three independent experiments. The significance of differences was determined through multiple comparisons with Dunnett's post hoc test at \*  $p < 0.05$  and \*\*  $p < 0.01$  compared with the indicated groups. LY294002, a PI3K inhibitor for reducing insulin signaling.

### 3.4. Overexpression of Nanog Protects Rat Brain against Aβ-Induced Cognitive Impairments

Finally, to investigate in vivo effects of Nanog-mediated neuroprotective potential against Aβ toxicity, we conducted an animal study based on intracerebral injection of Nanog expression vector into 12-week-old male Wistar rats. We stereotaxically delivered Nanog expression vector (rAAV-Nanog) into the brain ventricular space and Aβ<sub>1–42</sub> solutions were also stereotaxically injected bilaterally into hippocampus CA2 to imitate neurotoxic actions of Aβ [18]. First, to evaluate the mRNA and protein levels of Nanog, hippocampus and cortex were homogenized and evaluated by using qPCR. As shown in Figure 4b, qPCR analysis revealed that the injection of Nanog expressing vector in rats significantly increases Nanog mRNA levels (~10-fold) in hippocampus ( $p < 0.01$ ) and cortex ( $p < 0.05$ ).

Next, we examined whether exposure of rat hippocampal tissues to A $\beta$  contributes to insulin signaling blockage. As shown in Figure 4c, western blot analysis revealed that exposure of hippocampal tissues to A $\beta$  significantly induces IRS-1 Ser<sup>307</sup> and suppresses Akt Ser<sup>473</sup> phosphorylation, indicating that A $\beta$  can lead to neuronal insulin resistance. However, overexpression of Nanog resulted in effective restoration of this neuronal insulin resistance. To further assess cognitive flexibility, behavioral tests were also performed at 6 weeks after surgery for working and recognition memory by using T-maze and object recognition tests, respectively. As shown in Figure 4d, T-maze test results demonstrated that the A $\beta$ -only group shows a significantly low percentage of correct response, indicating A $\beta$  impairs spatial learning ( $F(3, 20) = 3.45, p < 0.05$ ). Conversely, a significant improvement was noted in the Nanog-overexpressed group. Latency to T-maze arm choice also exhibited similar results that the Nanog group features a shorter latency traveled before reaching the target of T-maze tests ( $F(3, 20) = 18.85, p < 0.01$ ). These observations were further confirmed with findings from experiments of object recognition test (Figure 4e), wherein the results showed that rats in the A $\beta$ -injected group spend significantly lower percentage of the time in exploring the novel object, indicating object recognition is damaged ( $F(3, 20) = 15.21, p < 0.01$ ). However, this recognition impairment was effectively restored in the Nanog-overexpressed group, suggesting that upregulation of Nanog in the brain may confer neuroprotection against A $\beta$ -induced cognitive deficits.

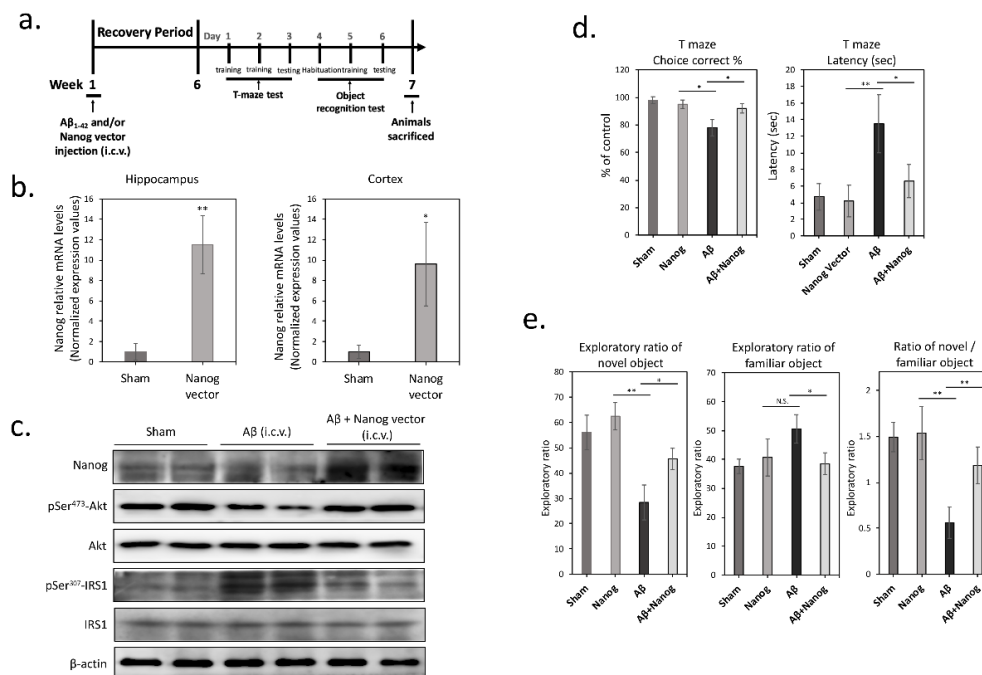


**Figure 4.** Upregulation of Nanog in rat brains improves working and recognition memory deficits induced by A $\beta$ . (a) The experimental protocol of the behavioral tests; (b) six weeks after stereotaxical injection, mRNA levels of Nanog were measured by performing qPCR. Nanog mRNA levels in hippocampus and cortex were significantly increased in Nanog-overexpressed group; (c) western blotting revealed that overexpression of Nanog markedly inhibited IRS-1 Ser<sup>307</sup> and restored Akt Ser<sup>473</sup> phosphorylation in rat hippocampus; (d) behavioral testing was performed at 6 weeks after stereotaxical surgery. Results showed the percentage of correct responses to select the arm with the reward and time latency to finish each session for the T-maze test; (e) percentage of time spent exploring new or old objects in object recognition test. Upregulation of Nanog in the brain significantly increased the ratio of novel/familiar object exploring time compared to A $\beta$ -injected group. Values were expressed as means  $\pm$  SEM from at least three independent experiments. The significance of differences was determined through unpaired Student's *t*-test or multiple comparisons with Dunnett's post hoc test at \*  $p < 0.05$  and \*\*  $p < 0.01$  compared with the indicated groups. N.S.: not significant.

#### 4. Discussion

Downregulation of insulin signaling in the brain was considered as an important feature in the pathogenesis of AD. In particular, defective neuronal insulin signaling is strongly linked to A $\beta$ -induced neurotoxicity [26]. In the brain, it is known that the insulin receptor is predominantly expressed in some specific regions including hippocampus, hypothalamus and cerebral cortex [27]. Notably, the principal role of insulin signaling in peripheral tissues is regulating the transport of glucose into the cell. However, researches have revealed that brain glucose uptake is not very greatly affected by insulin, suggesting insulin signaling may display some effects in the brain other than stimulation of glucose uptake [28]. In fact, numerous studies have demonstrated that brain insulin signaling is indeed involved in a broad spectrum of physiological functions. Especially in the hypothalamus, it is important for regulation of synaptic plasticity and long-term potentiation, two pathologic events occurring in AD progression [29]. As synaptic strength in the hippocampus is thought to be essential for the formation of spatial learning and memory, this indicates the dysfunction of neuronal insulin signaling may play a critical role in hippocampal synaptic plasticity impairment and cognitive decline. In contrast, restoration of insulin signaling can protect neurons from A $\beta$ -induced neurotoxicity. With that, our results demonstrated that A $\beta$  increases serine phosphorylation of IRS-1 and results in a concomitant reduction in Akt phosphorylation, consequently inhibiting insulin signaling in neuronal cells. On the contrary, overexpression of Nanog effectively attenuated A $\beta$ -induced insulin signaling blockade and, thereby, improved the cell viability by downregulating oxidative stress and apoptosis. Interestingly, GSK3 $\beta$  is known as a major kinase to induce abnormal tau hyperphosphorylation, which is another contributor to induce neuronal cell death in AD. Because Ser<sup>9</sup> phosphorylation is involved in the insulin signaling-mediated inhibition of GSK3 $\beta$  in neurons, A $\beta$ -induced neuronal insulin resistance is now recognized as a significant feature in the pathogenesis of AD [30]. Accordingly, our results also demonstrated overexpression of Nanog effectively suppresses A $\beta$ -induced tau phosphorylation and apoptosis by returning impaired neuronal insulin signaling. This further confirms that by increasing brain Nanog levels, insulin resistance and related cell death caused by A $\beta$  can be reduced.

In addition, we also found when cells were incubated with A $\beta$ , intracellular levels of Nanog was not inhibited by A $\beta$ . This indicates the downregulation of Nanog may not play a central role of the process of neurodegeneration in AD brains. Actually, the aging process in the brain increases the senescence and loss of neurons. Given that aging neuron may be a consequence with impaired insulin signaling by A $\beta$ , maintaining an efficient insulin sensitive in neurons can be a potential strategy for slowing neurodegeneration such as that seen in AD. As for how Nanog exerts its neuroprotection against A $\beta$  toxicity, we previously showed that Nanog maintains the self-renewal of neuronal cells through the insulin signaling pathway [14]. Some other studies also demonstrated that the transplantation of genetically modified neuronal cells to overexpress neurotrophic factors can improve synaptic plasticity and restore memory impairment in AD mice [31]. Since stem cells have been identified as an important source of neurotrophic factors secretion, it is believed that maintaining the stemness of damaged neuronal cells may help the treatment of AD [32]. In addition, a remarkable decline of hippocampal neurogenesis during the process of aging is observed *in vivo*, suggesting that the increase of stemness may promote neuronal precursor cells to differentiate into functional neurons [33]. Evidence has also demonstrated that insulin signaling is necessary for maintaining stem cell self-renewal and pluripotency [34]. Therefore, methods for increasing stem cell activity can be considered as a potential approach for replacing lost cells in degenerative diseases. Since our results showed that Nanog enhances a stem-like phenotype in human neuronal cells, the anti-A $\beta$  mechanism through which this occurs is worth to be used to inhibit disease progression of AD. For example, the use of some dietary phytochemical compounds that can stimulate Nanog expression may be applied in the future to develop the way in relieving A $\beta$ -induced neurotoxicity [35].

Cellular redox state is regulated by antioxidant signaling involves cellular enzymatic system to scavenge excessive ROS production. In our research, we found that the Nanog-associated ROS inhibition, especially inhibiting the superoxide from mitochondria seems largely composed of Nrf2-regulated

enzymes such SOD1 during A $\beta$  incubation. It is known that Nrf2 antioxidant signaling is particularly involved in the survival of hippocampal neural stem cells, and upregulation of Nrf2 in the aging brain can also mitigate neurogenic decline and improve cognitive abilities [36]. Since brain A $\beta$  deposition increases with age, these findings support our observations that activation of Nrf2 antioxidant system by Nanog may lead to a novel way for attenuating A $\beta$ -induced toxicity and senescence. In addition, co-activation of the Nrf2 and neurotrophic signaling pathway is shown to generate a synergistic effect in slowing AD progress [37]. This finding is consistent with our current results that both the Nrf2 antioxidant system and neurotrophic pathway activated by Nanog may confer synergistic benefits to attenuate A $\beta$  neurotoxicity. Because genetic manipulation of specific genes was shown to enhance antiaging properties of stem cells against exogenous stressors, upregulation of these genes such as Nanog involved in antioxidant restoration could be a feasible method to protect neurons from oxidative stress and associated damage [38]. Overall, the novelty of the present study lies in the cellular and behavioral analysis of Nanog's neuroprotection against A $\beta$ , as well as increased Nanog may be capable of supporting the survival and slowing aging of senescent neuronal cells. In conclusion, our results suggested a potential role for Nanog overexpression in modulating the neurotoxic effects of A $\beta$ , which implies that strategies to enhance insulin signaling by overexpression of Nanog could be used as an intervention for AD treatment.

**Author Contributions:** Conceptualization, C.-C.C., H.-H.L., T.-J.L., T.A.K., Y.-J.H. and C.-L.L.; methodology, H.-C.H., G.-Y.L. and Y.-J.H.; validation, C.-L.L.; investigation, C.-C.C., H.-H.L. and S.-H.T.; writing—original draft preparation, C.-C.C., H.-H.L. and S.-H.T.; writing—review and editing, T.A.K. and C.-L.L.; supervision, Y.-J.H.; project administration, C.-L.L.; funding acquisition, T.-J.L., Y.-J.H. and C.-L.L. All authors have read and agreed to the published version of the manuscript.

**Funding:** This work was supported by grants from the Chung Shan Medical University Hospital (CSH-2017-C-023), the National Chung Hsing University and Chung Shan Medical University (NCHU-CSMU-10603) and the Ministry of Science and Technology (106-2320-B-040-021-MY3, 108-2410-H-040-002-MY2, and 108-2320-B-040-029-MY2).

**Acknowledgments:** The fluorescence microscope and imaging analyzer were provided by the Instrument Center of Chung Shan Medical University, which is also supported by the Ministry of Science and Technology, Ministry of Education and Chung Shan Medical University.

**Conflicts of Interest:** The authors declare no conflict of interest. The funders had no role in the design of the study; in the collection, analyses or interpretation of data; in the writing of the manuscript or in the decision to publish the results.

## References

1. Chen, X.Q.; Mobley, W.C. Alzheimer Disease Pathogenesis: Insights From Molecular and Cellular Biology Studies of Oligomeric Abeta and Tau Species. *Front. Neurosci.* **2019**, *13*, 659. [[CrossRef](#)]
2. Lin, C.L.; Huang, W.N.; Li, H.H.; Huang, C.N.; Hsieh, S.; Lai, C.; Lu, F.J. Hydrogen-rich water attenuates amyloid beta-induced cytotoxicity through upregulation of Sirt1-FoxO3a by stimulation of AMP-activated protein kinase in SK-N-MC cells. *Chem. -Biol. Interact.* **2015**, *240*, 12–21. [[CrossRef](#)]
3. Marchant, N.L.; Reed, B.R.; Sanossian, N.; Madison, C.M.; Kriger, S.; Dhada, R.; Mack, W.J.; DeCarli, C.; Weiner, M.W.; Mungas, D.M.; et al. The aging brain and cognition: Contribution of vascular injury and abeta to mild cognitive dysfunction. *Jama Neurol.* **2013**, *70*, 488–495. [[CrossRef](#)]
4. Wei, Z.; Chen, X.C.; Song, Y.; Pan, X.D.; Dai, X.M.; Zhang, J.; Cui, X.L.; Wu, X.L.; Zhu, Y.G. Amyloid beta Protein Aggravates Neuronal Senescence and Cognitive Deficits in 5XFAD Mouse Model of Alzheimer's Disease. *Chin. Med. J.* **2016**, *129*, 1835–1844. [[CrossRef](#)]
5. Mecocci, P.; Boccardi, V.; Cecchetti, R.; Bastiani, P.; Scamosci, M.; Ruggiero, C.; Baroni, M. A Long Journey into Aging, Brain Aging, and Alzheimer's Disease Following the Oxidative Stress Tracks. *J. Alzheimer's Dis.* **2018**, *62*, 1319–1335. [[CrossRef](#)]
6. Sala Frigerio, C.; Wolfs, L.; Fattorelli, N.; Thrupp, N.; Voytyuk, I.; Schmidt, I.; Mancuso, R.; Chen, W.T.; Woodbury, M.E.; Srivastava, G.; et al. The Major Risk Factors for Alzheimer's Disease: Age, Sex, and Genes Modulate the Microglia Response to Abeta Plaques. *Cell Rep.* **2019**, *27*, 1293–1306. [[CrossRef](#)]
7. Gouras, G.K. Aging, Metabolism, Synaptic Activity, and Abeta in Alzheimer's Disease. *Front. Aging Neurosci.* **2019**, *11*, 185. [[CrossRef](#)]

8. Maciel-Baron, L.A.; Moreno-Blas, D.; Morales-Rosales, S.L.; Gonzalez-Puertos, V.Y.; Lopez-Diazguerrero, N.E.; Torres, C.; Castro-Obregon, S.; Konigsberg, M. Cellular Senescence, Neurological Function, and Redox State. *Antioxid. Redox Signal.* **2018**, *28*, 1704–1723. [[CrossRef](#)]
9. Fouad, G.I. Stem cells as a promising therapeutic approach for Alzheimer's disease: A review. *Bull. Natl. Res. Cent.* **2019**, *43*, 52. [[CrossRef](#)]
10. Ahmed Nel, M.; Murakami, M.; Hirose, Y.; Nakashima, M. Therapeutic Potential of Dental Pulp Stem Cell Secretome for Alzheimer's Disease Treatment: An In Vitro Study. *Stem. Cells Int.* **2016**, *2016*, 8102478. [[CrossRef](#)]
11. Griffith, C.M.; Eid, T.; Rose, G.M.; Patrylo, P.R. Evidence for altered insulin receptor signaling in Alzheimer's disease. *Neuropharmacology* **2018**, *136*, 202–215. [[CrossRef](#)]
12. Maciejczyk, M.; Zebrowska, E.; Chabowski, A. Insulin Resistance and Oxidative Stress in the Brain: What's New? *Int. J. Mol. Sci.* **2019**, *20*, 874. [[CrossRef](#)]
13. Bedse, G.; Di Domenico, F.; Serviddio, G.; Cassano, T. Aberrant insulin signaling in Alzheimer's disease: Current knowledge. *Front. Neurosci.* **2015**, *9*, 204. [[CrossRef](#)]
14. Li, H.H.; Lin, S.L.; Huang, C.N.; Lu, F.J.; Chiu, P.Y.; Huang, W.N.; Lai, T.J.; Lin, C.L. miR-302 Attenuates Amyloid-beta-Induced Neurotoxicity through Activation of Akt Signaling. *J. Alzheimer's Dis.* **2016**, *50*, 1083–1098. [[CrossRef](#)]
15. Kuijk, E.W.; van Mil, A.; Brinkhof, B.; Penning, L.C.; Colenbrander, B.; Roelen, B.A. PTEN and TRP53 independently suppress Nanog expression in spermatogonial stem cells. *Stem. Cells Dev.* **2010**, *19*, 979–988. [[CrossRef](#)]
16. Han, J.; Mistriotis, P.; Lei, P.; Wang, D.; Liu, S.; Andreadis, S.T. Nanog reverses the effects of organismal aging on mesenchymal stem cell proliferation and myogenic differentiation potential. *Stem Cells* **2012**, *30*, 2746–2759. [[CrossRef](#)]
17. Cheng, Y.W.; Chang, C.C.; Chang, T.S.; Li, H.H.; Hung, H.C.; Liu, G.Y.; Lin, C.L. Aβ stimulates microglial activation through antizyme-dependent downregulation of ornithine decarboxylase. *J. Cell. Physiol.* **2019**, *234*, 9733–9745. [[CrossRef](#)]
18. Lin, C.L.; Cheng, Y.S.; Li, H.H.; Chiu, P.Y.; Chang, Y.T.; Ho, Y.J.; Lai, T.J. Amyloid-beta suppresses AMP-activated protein kinase (AMPK) signaling and contributes to alpha-synuclein-induced cytotoxicity. *Exp. Neurol.* **2016**, *275 Pt 1*, 84–98. [[CrossRef](#)]
19. Huang, C.K.; Chang, Y.T.; Amstislavskaya, T.G.; Tikhonova, M.A.; Lin, C.L.; Hung, C.S.; Lai, T.J.; Ho, Y.J. Synergistic effects of ceftriaxone and erythropoietin on neuronal and behavioral deficits in an MPTP-induced animal model of Parkinson's disease dementia. *Behav. Brain. Res.* **2015**, *294*, 198–207. [[CrossRef](#)]
20. Toral-Rios, D.; Pichardo-Rojas, P.S.; Alonso-Vanegas, M.; Campos-Pena, V. GSK3β and Tau Protein in Alzheimer's Disease and Epilepsy. *Front. Cell. Neurosci.* **2020**, *14*, 19. [[CrossRef](#)]
21. Dinkova-Kostova, A.T.; Kostov, R.V.; Kazantsev, A.G. The role of Nrf2 signaling in counteracting neurodegenerative diseases. *FEBS J.* **2018**, *285*, 3576–3590. [[CrossRef](#)]
22. Chakravorty, A.; Jetto, C.T.; Manjithaya, R. Dysfunctional Mitochondria and Mitophagy as Drivers of Alzheimer's Disease Pathogenesis. *Front. Aging Neurosci.* **2019**, *11*, 311. [[CrossRef](#)]
23. Martinez-Cue, C.; Rueda, N. Cellular Senescence in Neurodegenerative Diseases. *Front. Cell. Neurosci.* **2020**, *14*, 16. [[CrossRef](#)]
24. Miranda, M.; Morici, J.F.; Zaroni, M.B.; Bekinschtein, P. Brain-Derived Neurotrophic Factor: A Key Molecule for Memory in the Healthy and the Pathological Brain. *Front. Cell. Neurosci.* **2019**, *13*, 363. [[CrossRef](#)]
25. Pardo, J.; Uriarte, M.; Console, G.M.; Reggiani, P.C.; Outeiro, T.F.; Morel, G.R.; Goya, R.G. Insulin-like growth factor-I gene therapy increases hippocampal neurogenesis, astrocyte branching and improves spatial memory in female aging rats. *Eur. J. Neurosci.* **2016**, *44*, 2120–2128. [[CrossRef](#)]
26. Lin, C.L.; Huang, C.N. The neuroprotective effects of the anti-diabetic drug linagliptin against Aβ-induced neurotoxicity. *Neural Regen. Res.* **2016**, *11*, 236–237. [[CrossRef](#)]
27. Lee, S.H.; Zabolotny, J.M.; Huang, H.; Lee, H.; Kim, Y.B. Insulin in the nervous system and the mind: Functions in metabolism, memory, and mood. *Mol. Metab.* **2016**, *5*, 589–601. [[CrossRef](#)]
28. Duarte, A.I.; Moreira, P.I.; Oliveira, C.R. Insulin in central nervous system: More than just a peripheral hormone. *J. Aging Res.* **2012**, *2012*, 384017. [[CrossRef](#)]
29. Spinelli, M.; Fusco, S.; Grassi, C. Brain Insulin Resistance and Hippocampal Plasticity: Mechanisms and Biomarkers of Cognitive Decline. *Front. Neurosci.* **2019**, *13*, 788. [[CrossRef](#)]

30. Rad, S.K.; Arya, A.; Karimian, H.; Madhavan, P.; Rizwan, F.; Koshy, S.; Prabhu, G. Mechanism involved in insulin resistance via accumulation of beta-amyloid and neurofibrillary tangles: Link between type 2 diabetes and Alzheimer's disease. *Drug Des. Dev.* **2018**, *12*, 3999–4021. [[CrossRef](#)]
31. Wu, C.C.; Lien, C.C.; Hou, W.H.; Chiang, P.M.; Tsai, K.J. Gain of BDNF Function in Engrafted Neural Stem Cells Promotes the Therapeutic Potential for Alzheimer's Disease. *Sci. Rep.* **2016**, *6*, 27358. [[CrossRef](#)]
32. Hosseini, S.A.; Mohammadi, R.; Noruzi, S.; Mohamadi, Y.; Azizian, M.; Mousavy, S.M.; Ghasemi, F.; Hesari, A.; Sahebkar, A.; Salarinia, R.; et al. Stem cell- and gene-based therapies as potential candidates in Alzheimer's therapy. *J. Cell Biochem.* **2018**, *119*, 8723–8736. [[CrossRef](#)]
33. Apple, D.M.; Solano-Fonseca, R.; Kokovay, E. Neurogenesis in the aging brain. *Biochem. Pharm.* **2017**, *141*, 77–85. [[CrossRef](#)]
34. Teng, C.F.; Jeng, L.B.; Shyu, W.C. Role of Insulin-like Growth Factor 1 Receptor Signaling in Stem Cell Stemness and Therapeutic Efficacy. *Cell Transpl.* **2018**, *27*, 1313–1319. [[CrossRef](#)]
35. Sarubbo, F.; Moranta, D.; Pani, G. Dietary polyphenols and neurogenesis: Molecular interactions and implication for brain ageing and cognition. *Neurosci. Biobehav. Rev.* **2018**, *90*, 456–470. [[CrossRef](#)]
36. Ray, S.; Corenblum, M.J.; Anandhan, A.; Reed, A.; Ortiz, F.O.; Zhang, D.D.; Barnes, C.A.; Madhavan, L. A Role for Nrf2 Expression in Defining the Aging of Hippocampal Neural Stem Cells. *Cell Transpl.* **2018**, *27*, 589–606. [[CrossRef](#)]
37. Murphy, K.E.; Park, J.J. Can Co-Activation of Nrf2 and Neurotrophic Signaling Pathway Slow Alzheimer's Disease? *Int. J. Mol. Sci.* **2017**, *18*, 1168. [[CrossRef](#)]
38. Brookhouser, N.; Tekel, S.J.; Standage-Beier, K.; Nguyen, T.; Schwarz, G.; Wang, X.; Brafman, D.A. BIG-TREE: Base-Edited Isogenic hPSC Line Generation Using a Transient Reporter for Editing Enrichment. *Stem Cell Rep.* **2020**, *14*, 184–191. [[CrossRef](#)]



© 2020 by the authors. Licensee MDPI, Basel, Switzerland. This article is an open access article distributed under the terms and conditions of the Creative Commons Attribution (CC BY) license (<http://creativecommons.org/licenses/by/4.0/>).